Eur. Phys. J. C (2012) 72:1972
DOI 10.1140/epjc/s10052-012-1972-7

THE EUROPEAN PHYSICAL JOURNAL C

Letter

Observation of $X(3872)$ production in pp collisions at $\sqrt{s} = 7$ TeV

The LHCb Collaboration*
CERN, 1211 Geneva 23, Switzerland

Received: 23 December 2011 / Revised: 23 March 2012 / Published online: 4 May 2012

Abstract Using 34.7 pb^{-1} of data collected with the LHCb detector, the inclusive production of the $X(3872)$ meson in pp collisions at $\sqrt{s} = 7$ TeV is observed for the first time. Candidates are selected in the $X(3872) \to J/\psi\pi^+\pi^-$ decay mode, and used to measure

$$\sigma\big(pp \to X(3872) + \text{anything}\big)\mathcal{B}\big(X(3872) \to J/\psi\pi^+\pi^-\big) = 5.4 \pm 1.3\ (\text{stat}) \pm 0.8\ (\text{syst})\ \text{nb},$$

where $\sigma(pp \to X(3872) + \text{anything})$ is the inclusive production cross section of $X(3872)$ mesons with rapidity in the range 2.5–4.5 and transverse momentum in the range 5–20 GeV/c. In addition the masses of both the $X(3872)$ and $\psi(2S)$ mesons, reconstructed in the $J/\psi\pi^+\pi^-$ final state, are measured to be

$$m_{X(3872)} = 3871.95 \pm 0.48\ (\text{stat}) \pm 0.12\ (\text{syst})\ \text{MeV}/c^2$$

and

$$m_{\psi(2S)} = 3686.12 \pm 0.06\ (\text{stat}) \pm 0.10\ (\text{syst})\ \text{MeV}/c^2.$$

1 Introduction

The $X(3872)$ particle was discovered in 2003 by the Belle collaboration in the $B^\pm \to X(3872)K^\pm$, $X(3872) \to J/\psi\pi^+\pi^-$ decay chain [1]. Its existence was confirmed by the CDF [2], DØ [3] and BaBar [4] collaborations. The discovery of the $X(3872)$ particle and the subsequent observation of several other new states in the mass range 3.9–4.7 GeV/c^2 have led to a resurgence of interest in exotic meson spectroscopy [5].

Several properties of the $X(3872)$ have been determined, in particular its mass [6–8] and the dipion mass spectrum in the decay $X(3872) \to J/\psi\pi^+\pi^-$ [7, 9], but its quantum numbers, which have been constrained to be either $J^{PC} = 2^{-+}$ or 1^{++} [10], are still not established. Despite a large experimental effort, the nature of this new state is still uncertain and several models have been proposed to describe it. The $X(3872)$ could be a conventional charmonium state, with one candidate being the $\eta_{c2}(1D)$ meson [5]. However, the mass of this state is predicted to be far below the observed $X(3872)$ mass. Given the proximity of the $X(3872)$ mass to the $D^{*0}\bar{D}^0$ threshold, another possibility is that the $X(3872)$ is a loosely bound $D^{*0}\bar{D}^0$ 'molecule', i.e. a $((u\bar{c})(c\bar{u}))$ system [5]. For this interpretation to be valid the mass of the $X(3872)$ should be less than the sum of D^{*0} and D^0 masses. A further, more exotic, possibility is that the $X(3872)$ is a tetraquark state [11].

Measurements of $X(3872)$ production at hadron colliders, where most of the production is prompt rather than from b-hadron decays, may shed light on the nature of this particle. In particular, it has been discussed whether or not the possible molecular nature of the $X(3872)$ is compatible with the production rate observed at the Tevatron [12, 13]. Predictions for $X(3872)$ production at the LHC have also been published [13].

This paper reports an observation of $X(3872)$ production in pp collisions at $\sqrt{s} = 7$ TeV using an integrated luminosity of 34.7 pb^{-1} collected by the LHCb experiment. The $X(3872) \to J/\psi\pi^+\pi^-$ selection is optimized on the similar but more abundant $\psi(2S) \to J/\psi\pi^+\pi^-$ decay. The observed $X(3872)$ signal is used to measure both the $X(3872)$ mass and the production rate from all sources including b-hadron decays, i.e. the absolute inclusive $X(3872)$ production cross section in the detector acceptance multiplied by the $X(3872) \to J/\psi\pi^+\pi^-$ branching fraction.

2 The LHCb spectrometer and data sample

The LHCb detector is a forward spectrometer [14] at the Large Hadron Collider (LHC). It provides reconstruction of charged particles in the pseudorapidity range $2 < \eta < 5$. The detector elements are placed along the LHC beam line

* e-mail: joel.bressieux@epfl.ch

starting with the vertex detector (VELO), a silicon strip device that surrounds the proton-proton interaction region. It is used to reconstruct both the interaction vertices and the decay vertices of long-lived hadrons. It also contributes to the measurement of track momenta, along with a large area silicon strip detector located upstream of a dipole magnet and a combination of silicon strip detectors and straw drift-tubes placed downstream. The magnet has a bending power of about 4 Tm. The combined tracking system has a momentum resolution $\delta p/p$ that varies from 0.4 % at 5 GeV/c to 0.6 % at 100 GeV/c. Two ring imaging Cherenkov (RICH) detectors are used to identify charged hadrons. The detector is completed by electromagnetic calorimeters for photon and electron identification, a hadron calorimeter, and a muon system consisting of alternating layers of iron and multi-wire proportional chambers. The trigger consists of a hardware stage, based on information from the calorimeter and muon systems, followed by a software stage which applies a full event reconstruction.

The cross-section analysis described in this paper is based on a data sample collected in 2010, exclusively using events that passed dedicated J/ψ trigger algorithms. These algorithms selected a pair of oppositely charged muon candidates, where either one of the muons had a transverse momentum p_{T} larger than 1.8 GeV/c or one of the two muons had $p_{\mathrm{T}} > 0.56$ GeV/c and the other $p_{\mathrm{T}} > 0.48$ GeV/c. The pair of muons was required to originate from a common vertex and have an invariant mass in a wide window around the J/ψ mass. The $X(3872)$ mass measurement also uses events triggered with other algorithms, such as single-muon triggers. To avoid domination of the trigger CPU time by a few events with high occupancy, a set of cuts was applied on the hit multiplicity of each sub-detector used by the pattern recognition algorithms. These cuts reject high-multiplicity events with a large number of pp interactions.

The accuracy of the $X(3872)$ mass measurement relies on the calibration of the tracking system [15]. The spatial alignment of the tracking detectors, as well as the calibration of the momentum scale, are based on the $J/\psi \to \mu^+\mu^-$ mass peak. This was carried out in seven time periods corresponding to known changes in the detector running conditions. The procedure takes into account the effects of QED radiative corrections which are important in this decay.

The analysis uses fully simulated samples based on the PYTHIA 6.4 generator [16] configured with the parameters detailed in [17]. The EVTGEN [18], PHOTOS [19] and GEANT4 [20] packages are used to describe the decays of unstable particles, model QED radiative corrections and simulate interactions in the detector, respectively. The $X(3872) \to J/\psi\pi^+\pi^-$ Monte Carlo events are generated assuming that the ρ resonance dominates the dipion mass spectrum, as established by the CDF [9] and Belle [7] data.

3 Event selection

To isolate the $X(3872)$ signal, tight cuts are needed to reduce combinatorial background where a correctly reconstructed J/ψ meson is combined with a random $\pi^+\pi^-$ pair from the primary pp interaction. The cuts are defined using reconstructed $\psi(2S) \to J/\psi\pi^+\pi^-$ decays, as well as 'same-sign pion' candidates satisfying the same criteria as used for the $X(3872)$ and $\psi(2S)$ selection but where the two pions have the same electric charge. The Kullback–Leibler (KL) distance [21–23] is used to suppress duplicated particles created by the reconstruction: if two particles have a symmetrized KL divergence less than 5000, only that with the higher track fit quality is considered.

$J/\psi \to \mu^+\mu^-$ candidates are formed from pairs of oppositely charged particles identified as muons, originating from a common vertex with a χ^2 per degree of freedom (χ^2/ndf) smaller than 20, and with an invariant mass in the range 3.04–3.14 GeV/c^2. The two muons are each required to have a momentum above 10 GeV/c and a transverse momentum above 1 GeV/c. To reduce background from the decay in flight of pions and kaons, each muon candidate is required to have a track fit χ^2/ndf less than 4. Finally J/ψ candidates are required to have a transverse momentum larger than 3.5 GeV/c.

Pairs of oppositely charged pions are combined with J/ψ candidates to build $\psi(2S)$ and $X(3872)$ candidates. To reduce the combinatorial background, each pion candidate is required to have a transverse momentum above 0.5 GeV/c and a track fit χ^2/ndf less than 4. In addition, kaons are removed using the RICH information by requiring the likelihood for the kaon hypothesis to be smaller than that for the pion hypothesis. A vertex fit is performed [24] that constrains the four daughter particles to originate from a common point and the mass of the muon pair to the nominal J/ψ mass [25]. This fit both improves the mass resolution and reduces the sensitivity of the result to the momentum scale calibration. To further reduce the combinatorial background the χ^2/ndf of this fit is required to be less than 5. Finally, the requirement $Q < 300$ MeV/c^2 is applied where $Q = M_{\mu\mu\pi\pi} - M_{\mu\mu} - M_{\pi\pi}$, and $M_{\mu\mu\pi\pi}$, $M_{\mu\mu}$ and $M_{\pi\pi}$ are the reconstructed masses before any mass constraint; this requirement removes 35 % of the background whilst retaining 97 % of the $X(3872)$ signal.

Figure 1 shows the $J/\psi\pi^+\pi^-$ mass distribution for the selected candidates, with clear signals for both the $\psi(2S)$ and the $X(3872)$ mesons, as well as the $J/\psi\pi^\pm\pi^\pm$ mass distribution of the same-sign pion candidates.

4 Mass measurements

The masses of the $\psi(2S)$ and $X(3872)$ mesons are determined from an extended unbinned maximum likelihood

fit of the reconstructed $J/\psi\pi^+\pi^-$ mass in the interval $3.60 < M_{J/\psi\pi\pi} < 3.95$ GeV/c^2. The $\psi(2S)$ and $X(3872)$ signals are each described with a non-relativistic Breit–Wigner function convolved with a Gaussian resolution function. The intrinsic width of the $\psi(2S)$ is fixed to the PDG value, $\Gamma_{\psi(2S)} = 0.304$ MeV/c^2 [25]. The Belle collaboration recently reported [7] that the $X(3872)$ width is less than 1.2 MeV/c^2 at 90 % confidence level; we fix the $X(3872)$ width to zero in the nominal fit. The ratio of the mass resolutions for the $X(3872)$ and the $\psi(2S)$ is fixed to the value estimated from the simulation, $\sigma^{\rm MC}_{X(3872)}/\sigma^{\rm MC}_{\psi(2S)} = 1.31$.

Studies using the same-sign pion candidates show that the background shape can be described by the functional form $f(M) \propto (M - m_{\rm th})^{c_0}\exp(-c_1 M - c_2 M^2)$, where $m_{\rm th} = m_{J/\psi} + 2m_\pi = 3376.05$ MeV/c^2 [25] is the mass threshold and c_0, c_1 and c_2 are shape parameters. To improve the stability of the fit, the parameter c_2 is fixed to the value obtained from the same-sign pion sample.

In total, the fit has eight free parameters: three yields ($\psi(2S)$, $X(3872)$ and background), two masses ($\psi(2S)$ and $X(3872)$), one resolution parameter, and two background shape parameters. The correctness of the fitting procedure has been checked with simplified Monte Carlo samples, fully simulated Monte Carlo samples, and samples containing a mixture of fully simulated Monte Carlo signal events and same-sign background events taken from the data. The fit results are shown in Fig. 1 and Table 1. The fit does not account for QED radiative corrections and hence underestimates the masses. Using a simulation based on PHOTOS [19] the biases on the $X(3872)$ and $\psi(2S)$ masses are found to be -0.07 ± 0.02 MeV/c^2 and -0.02 ± 0.02 MeV/c^2, respectively. The fitted mass values are corrected for these biases and the uncertainties propagated in the estimate of the systematic error.

Several other sources of systematic effects on the mass measurements are considered. For each source, the complete analysis is repeated (including the track fit and the momentum scale calibration when needed) under an alternative assumption, and the observed change in the central value of the fitted masses relative to the nominal results assigned as a systematic uncertainty. The dominant source of uncertainty is the calibration of the momentum scale. Based on checks performed with reconstructed signals of various mesons decaying into two-body final states (such as $\pi^+\pi^-$, $K^\mp\pi^\pm$ and $\mu^+\mu^-$) a relative systematic uncertainty of 0.02 % is assigned to the momentum scale [15], which translates into a 0.10 (0.08) MeV/c^2 uncertainty on the $X(3872)$ ($\psi(2S)$) mass. After the calibration procedure with the $J/\psi \to \mu^+\mu^-$ decay, a ± 0.07 % variation of the momentum scale remains as a function of the particle pseudorapidity η. To first order this effect averages out in the mass determination. The residual impact of this variation is evaluated by parameterizing the momentum scale as function of η and repeating the analysis. The systematic uncertainty associated with the momentum calibration indirectly takes into account any effect related to the imperfect alignment of the tracking stations. However, the alignment of the VELO may affect the mass measurements through the determination of the horizontal and vertical slopes of the tracks. This is investigated by changing the track slopes by amounts corresponding to the 0.1 % relative precision with which the length scale along the beam axis is known [26]. Other small uncertainties arise due to the limited knowledge of the $X(3872)$ width and the modeling of the resolution. The former is estimated by fixing the $X(3872)$ width to 0.7 MeV/c^2 instead of zero, as suggested by the likelihood published by Belle [7]. The latter is estimated by fixing the ratio $\sigma_{X(3872)}/\sigma_{\psi(2S)}$ using the covariance estimates

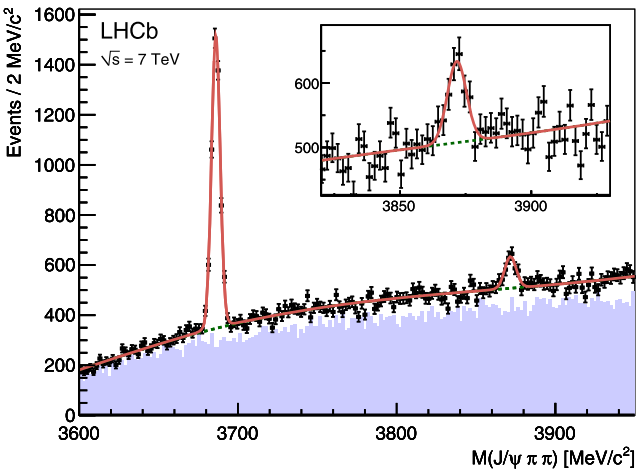

Fig. 1 Invariant mass distribution of $J/\psi\pi^+\pi^-$ (*points with statistical error bars*) and same-sign $J/\psi\pi^\pm\pi^\pm$ (*filled histogram*) candidates. *The curves* are the result of the fit described in the text. *The inset* shows a zoom of the $X(3872)$ region

Table 1 Results of the fit to the $J/\psi\pi^+\pi^-$ invariant mass distribution of Fig. 1

Fit parameter or derived quantity	$\psi(2S)$	$X(3872)$
Number of signal events	3998 ± 83	565 ± 62
Mass m [MeV/c^2]	3686.10 ± 0.06	3871.88 ± 0.48
Resolution σ [MeV/c^2]	2.54 ± 0.06	3.33 ± 0.08
Signal-to-noise ratio in $\pm 3\sigma$ window	1.5	0.15
Number of background events	73094 ± 282	

Table 2 Systematic uncertainties on the $\psi(2S)$ and $X(3872)$ mass measurements

Category	Source of uncertainty	Δm [MeV/c^2]	
		$\psi(2S)$	$X(3872)$
Mass fitting	Natural width	–	0.01
	Radiative tail	0.02	0.02
	Resolution	–	0.01
	Background model	0.02	0.02
Momentum calibration	Average momentum scale	0.08	0.10
	η dependence of momentum scale	0.02	0.03
Detector description	Energy loss correction	0.05	0.05
Detector alignment	Track slopes	0.01	0.01
Total		0.10	0.12

returned by the track fit algorithm on signal events in the data sample, rather than using the mass resolutions from the simulation. The effect of background modeling is estimated by performing the fit on two large samples, one with only Monte Carlo signal events, and one containing a mixture of Monte Carlo signal events and background candidates obtained by combining a J/ψ candidate and a same-sign pion pair from different data events: the difference in the fitted mass values is taken as a systematic uncertainty. The amount of material traversed in the tracking system by a particle is estimated to be known to a 10 % accuracy [27]; the magnitude of the energy loss correction in the reconstruction is therefore varied by 10 %. The assigned systematic uncertainties are summarized in Table 2 and combined in quadrature.

Systematic checks of the stability of the measured $\psi(2S)$ mass are performed, splitting the data sample according to different run periods or to the dipole magnet polarity, or ignoring the hits from the tracking station before the magnet. In addition, the measurement is repeated in bins of the p, p_{T} and Q values of the $\psi(2S)$ signal. No evidence for a systematic bias is found.

5 Determination of the production cross section

The observed $X(3872)$ signal is used to measure the product of the inclusive production cross section $\sigma(pp \to X(3872) + \text{anything})$ and the branching fraction $\mathcal{B}(X(3872) \to J/\psi\pi^+\pi^-)$, according to

$$\sigma\left(pp \to X(3872) + \text{anything}\right)\mathcal{B}\left(X(3872) \to J/\psi\pi^+\pi^-\right) = \frac{N^{\mathrm{corr}}_{X(3872)}}{\xi\,\mathcal{B}(J/\psi \to \mu^+\mu^-)\mathcal{L}_{\mathrm{int}}}, \quad (1)$$

where $N^{\mathrm{corr}}_{X(3872)}$ is the efficiency-corrected signal yield, ξ is a correction factor to the simulation-derived efficiency that accounts for known differences between data and simulation, $\mathcal{B}(J/\psi \to \mu^+\mu^-) = (5.93 \pm 0.06)$ % [25] is the $J/\psi \to \mu^+\mu^-$ branching fraction, and $\mathcal{L}_{\mathrm{int}}$ is the integrated luminosity.

The absolute luminosity scale was measured at specific periods during the 2010 data taking [28] using both Van der Meer scans [29] and a beam-gas imaging method [30]. The instantaneous luminosity determination is then based on a continuous recording of the multiplicity of tracks in the VELO, which has been normalized to the absolute luminosity scale [28]. The integrated luminosity of the sample used in this analysis is determined to be $\mathcal{L}_{\mathrm{int}} = 34.7 \pm 1.2\ \mathrm{pb}^{-1}$, with an uncertainty dominated by the knowledge of the beam currents.

Only $X(3872)$ candidates for which the J/ψ triggered the event are considered, keeping 70 % of the raw signal yield used for the mass measurement. In addition, the candidates are required to lie inside the fiducial region for the measurement,

$$2.5 < y < 4.5 \quad \text{and} \quad 5 < p_{\mathrm{T}} < 20\ \mathrm{GeV}/c, \quad (2)$$

where y and p_{T} are the rapidity and transverse momentum of the $X(3872)$. This region provides a good balance between a high efficiency (92 % of the triggered events) and a low systematic uncertainty on the acceptance correction.

The corrected yield $N^{\mathrm{corr}}_{X(3872)} = 9140 \pm 2224$ is obtained from a mass fit in the narrow region 3820–3950 MeV/c^2, with a linear background model and the same $X(3872)$ signal model as used previously but with the mass and resolution fixed to the central values presented in Sect. 4. In this fit, each candidate is given a weight equal to the reciprocal of the total signal efficiency estimated from simulation for the y and p_{T} of that candidate. A second method based on the sWeight [31] technique was found to give consistent results. The average total signal efficiency in the fiducial region of (2) is estimated to be $N_{X(3872)}/N^{\mathrm{corr}}_{X(3872)} = 4.2$ %, where $N_{X(3872)}$ is the observed signal yield obtained from a mass fit without weighting the events. This low value of the efficiency is driven by the geometrical acceptance and the requirement on the p_{T} of the J/ψ meson.

The quantity ξ of (1) is the product of three factors. The first two, 1.024 ± 0.011 [32] and 0.869 ± 0.043, account for differences between the data and simulation for the efficiency of the muon and pion identifications, respectively. The third factor, 0.92 ± 0.03, corresponds to the efficiency of the hit-multiplicity cuts applied in the trigger, which is not accounted for in the simulation. It is obtained from a fit of the distribution of the number of hits in the VELO.

The relative systematic uncertainties assigned to the cross-section measurement are listed in Table 3, and quadratically add up to 14.2 %. The cross-section measurement is performed under the most favored assumption for the quantum numbers of the $X(3872)$ particle, $J^{PC} = 1^{++}$ [33], which is used for the generation of Monte Carlo events. No systematic uncertainty is assigned to cover other cases. Besides the uncertainties already mentioned on $\mathcal{B}(J/\psi \to \mu^+\mu^-)$, $\mathcal{L}_{\rm int}$ and ξ, the following sources of systematics on $N^{\rm corr}_{X(3872)}$ are considered. The dominant uncertainty is due to differences in the efficiency of track reconstruction between the data and simulation. This is estimated to be 7.4 % using a data driven tag and probe approach based on $J/\psi \to \mu^+\mu^-$ candidates. An additional uncertainty of 0.5 % per track is assigned to cover differences in the efficiency of the track χ^2/ndf cut between data and simulation. Similarly, a 3 % uncertainty is assigned due to the effect of the vertex χ^2 cuts.

Other important sources of uncertainty are due to the modeling of the signal and background mass distributions. Repeating the mass fit with the $X(3872)$ decay width fixed to 0.7 MeV/c^2 instead of zero results in a 5 % change of the signal yield. Similarly, the uncertainties due to the $X(3872)$ mass resolution are estimated by repeating the mass fit with different fixed mass resolutions: first changing it by the statistical uncertainty reported in Table 1, and then changing it by the systematic uncertainty resulting from the knowledge of the resolution ratio $\sigma_{X(3872)}/\sigma_{\psi(2S)}$, as described in Sect. 4. The combined effect on the $X(3872)$ signal yield corresponds to a 2.5 % systematic uncertainty.

Using an exponential rather than linear function to describe the background leads to a change of 6.4 % in signal yield, which is taken as an additional systematic uncertainty.

The unknown $X(3872)$ polarization affects the total efficiency, mainly through the J/ψ reconstruction efficiency. The dipion system is less affected, in particular the efficiency is found to be constant as a function of the dipion mass. The simulation efficiency, determined assuming no J/ψ polarization, is recomputed in two extreme schemes for the J/ψ polarization (fully transverse and fully longitudinal) [32] and the maximum change of 2.1 % is taken as systematic uncertainty. The efficiency of the Q cut depends on the $X(3872)$ decay model. The dipion mass spectrum obtained in this analysis does not have enough accuracy to discriminate between reasonable models. Comparing the results obtained with the $X(3872) \to J/\psi\rho$ decay models used by CDF [9] and by Belle [7], we evaluated a 1 % systematic uncertainty on the Q-cut efficiency.

Finally, differences in the trigger efficiency between data and simulation are studied using events triggered independently of the J/ψ candidate. Based on these studies an uncertainty of 2.9 % is assigned.

Table 3 Relative systematic uncertainties on the $X(3872)$ production cross-section measurement. The total uncertainty is the quadratic sum of the individual contributions

Source of uncertainty	$\Delta\sigma/\sigma$ [%]
$X(3872)$ polarization	2.1
$X(3872)$ decay model	1.0
$X(3872)$ decay width	5.0
Mass resolution	2.5
Background model	6.4
Tracking efficiency	7.4
Track χ^2 cut	2.0
Vertex χ^2 cut	3.0
Muon trigger efficiency	2.9
Hit-multiplicity cuts	3.0
Muon identification	1.1
Pion identification	4.9
Integrated luminosity	3.5
$J/\psi \to \mu^+\mu^-$ branching fraction	1.0
Total	14.2

6 Results and conclusion

With an integrated luminosity of 34.7 pb^{-1} collected by the LHCb experiment, the production of the $X(3872)$ particle is observed in pp collisions at $\sqrt{s} = 7$ TeV. The product of the production cross section and the branching ratio into $J/\psi\pi^+\pi^-$ is

$$\sigma\big(pp \to X(3872) + \text{anything}\big)\mathcal{B}\big(X(3872) \to J/\psi\pi^+\pi^-\big) = 5.4 \pm 1.3\ (\text{stat}) \pm 0.8\ (\text{syst})\ \text{nb},$$

for $X(3872)$ mesons produced (either promptly or from the decay of other particles) with a rapidity between 2.5 and 4.5 and a transverse momentum between 5 and 20 GeV/c.

Predictions for the $X(3872) \to J/\psi\pi^+\pi^-$ production at the LHC are available from a non-relativistic QCD model which assumes that the cross section is dominated by the production of charm quark pairs with negligible relative momentum [13]. The calculations are normalized using extrapolations from measurements performed at the Tevatron. When restricted to the kinematic range of our measurement and summed over prompt production and production from

b-hadron decays, the results of [13] yield 13.0 ± 2.7 nb, where the quoted uncertainty originates from the experimental input used in the calculation. This prediction exceeds our measurement by 2.4σ.

After calibration using $J/\psi \to \mu^+\mu^-$ decays, the masses of both the $X(3872)$ and $\psi(2S)$ mesons, reconstructed in the same $J/\psi\pi^+\pi^-$ final state, are measured to be

$$m_{X(3872)} = 3871.95 \pm 0.48\ (\text{stat}) \pm 0.12\ (\text{syst})\ \text{MeV}/c^2,$$

$$m_{\psi(2S)} = 3686.12 \pm 0.06\ (\text{stat}) \pm 0.10\ (\text{syst})\ \text{MeV}/c^2,$$

in agreement with the current world averages [25], and with the recent $X(3872)$ mass measurement from Belle [7]. The measurements of the $X(3872)$ mass are consistent, within uncertainties, with the sum of the D^0 and D^{*0} masses, $3871.79 \pm 0.29\ \text{MeV}/c^2$, computed from the results of the global PDG fit of the charm meson masses [25].

Acknowledgements We thank P. Artoisenet and E. Braaten for useful discussions and for recomputing the numerical prediction of [13] in the fiducial region of our measurement. We express our gratitude to our colleagues in the CERN accelerator departments for the excellent performance of the LHC. We thank the technical and administrative staff at CERN and at the LHCb institutes, and acknowledge support from the National Agencies: CAPES, CNPq, FAPERJ and FINEP (Brazil); CERN; NSFC (China); CNRS/IN2P3 (France); BMBF, DFG, HGF and MPG (Germany); SFI (Ireland); INFN (Italy); FOM and NWO (The Netherlands); SCSR (Poland); ANCS (Romania); MinES of Russia and Rosatom (Russia); MICINN, XuntaGal and GENCAT (Spain); SNSF and SER (Switzerland); NAS Ukraine (Ukraine); STFC (United Kingdom); NSF (USA). We also acknowledge the support received from the ERC under FP7 and the Region Auvergne.

References

1. S.-K. Choi et al. (Belle collaboration), Observation of a new narrow charmonium state in exclusive $B^+ \to K^\pm\pi^+\pi^- J/\psi$ decays. Phys. Rev. Lett. **91**, 262001 (2003). arXiv:hep-ex/0309032
2. D. Acosta et al. (CDF collaboration), Observation of the narrow state $X(3872) \to J/\psi\pi^+\pi^-$ in $p\bar{p}$ collisions at $\sqrt{s} = 1.96$ TeV. Phys. Rev. Lett. **93**, 072001 (2004). arXiv:hep-ex/0312021
3. V.M. Abazov et al. (DØ collaboration), Observation and properties of the $X(3872)$ decaying to $J/\psi\pi^+\pi^-$ in $p\bar{p}$ collisions at $\sqrt{s} =$ 1.96 TeV. Phys. Rev. Lett. **93**, 162002 (2004). arXiv:hep-ex/0405004
4. B. Aubert et al. (BaBar collaboration), Study of the $B^- \to J/\psi K^-\pi^+\pi^-$ decay and measurement of the $B^- \to X(3872)K^-$ branching fraction. Phys. Rev. D **71**, 071103 (2005). arXiv:hep-ex/0406022
5. E. Swanson, The new heavy mesons: a status report. Phys. Rep. **429**, 243 (2006). arXiv:hep-ph/0601110
6. T. Aaltonen et al. (CDF collaboration), Precision measurement of the $X(3872)$ mass in $J/\psi\pi^+\pi^-$ decays. Phys. Rev. Lett. **103**, 152001 (2009). arXiv:0906.5218
7. S.-K. Choi et al. (Belle collaboration), Bounds on the width, mass difference and other properties of $X(3872) \to \pi^+\pi^- J/\psi$ decays. Phys. Rev. D **84**, 052004 (2011). arXiv:1107.0163
8. B. Aubert et al. (BaBar collaboration), A study of $B \to X(3872)K$, with $X(3872) \to J/\psi\pi^+\pi^-$. Phys. Rev. D **77**, 111101 (2008). arXiv:0803.2838
9. A. Abulencia et al. (CDF collaboration), Measurement of the dipion mass spectrum in $X(3872) \to J/\psi\pi^+\pi^-$ decays. Phys. Rev. Lett. **96**, 102002 (2006). arXiv:hep-ex/0512074
10. A. Abulencia et al. (CDF collaboration), Analysis of the quantum numbers J^{PC} of the $X(3872)$. Phys. Rev. Lett. **98**, 132002 (2007). arXiv:hep-ex/0612053
11. L. Maiani, F. Piccinini, A.D. Polosa, V. Riquer, Diquark-antidiquarks with hidden or open charm and the nature of $X(3872)$. Phys. Rev. D **71**, 014028 (2005). arXiv:hep-ph/0412098
12. C. Bignamini, B. Grinstein, F. Piccinini, A.D. Polosa, C. Sabelli, Is the $X(3872)$ production cross section at $\sqrt{s} = 1.96$ TeV compatible with a hadron molecule interpretation. Phys. Rev. Lett. **103**, 162001 (2009). arXiv:0906.0882
13. P. Artoisenet, E. Braaten, Production of the $X(3872)$ at the Tevatron and the LHC. Phys. Rev. D **81**, 114018 (2010). arXiv:0911.2016
14. A.A. Alves Jr et al. (LHCb collaboration), The LHCb detector at the LHC. J. Instrum. **3**, S08005 (2008)
15. R. Aaij et al. (LHCb collaboration), Measurement of b-hadron masses. Phys. Lett. B **708**, 241 (2012). arXiv:1112.4896
16. T. Sjöstrand, S. Mrenna, P. Skands, PYTHIA 6.4 physics and manual. J. High Energy Phys. **05**, 026 (2006). arXiv:hep-ph/0603175
17. I. Belyaev et al., Handling of the generation of primary events in GAUSS, the LHCb simulation framework, in *Nuclear Science Symposium Conference Record (NSS/MIC)* (IEEE Press, New York, 2010), p. 1155
18. D.J. Lange, The EvtGen particle decay simulation package. Nucl. Instrum. Methods, Sect. A **462**, 152 (2001)
19. E. Barberio, Z. Wąs, PHOTOS—a universal Monte Carlo for QED radiative corrections: version 2.0. Comput. Phys. Commun. **79**, 291 (1994)
20. S. Agostinelli et al. (GEANT4 collaboration), GEANT4—a simulation toolkit. Nucl. Instrum. Methods, Sect. A **506**, 250 (2003)
21. S. Kullback, R.A. Leibler, On information and sufficiency. Ann. Math. Stat. **22**, 79 (1951)
22. S. Kullback, Letter to editor: the Kullback–Leibler distance. Am. Stat. **41**, 340 (1987)
23. M. Needham, Clone track identification using the Kullback–Leibler distance, LHCb-2008-002 (The use of the Kullback–Leibler distance is described)
24. W.D. Hulsbergen, Decay chain fitting with a Kalman filter. Nucl. Instrum. Methods, Sect. A **552**, 566 (2005). arXiv:physics/0503191
25. K. Nakamura et al. (Particle Data Group), Review of particle physics. J. Phys. G **37**, 075021 (2010)
26. R. Aaij et al. (LHCb collaboration), Measurement of the $B_s^0 - \bar{B}_s^0$ oscillation frequency Δm_s in $B_s^0 \to D_s^-(3)\pi$ decays. Phys. Lett. B **709**, 177 (2012). arXiv:1112.4311
27. R. Aaij et al. (LHCb collaboration), Prompt K_S^0 production in pp collisions at $\sqrt{s} = 0.9$ TeV. Phys. Lett. B **693**, 69 (2010). arXiv:1008.3105
28. R. Aaij et al. (LHCb collaboration), Absolute luminosity measurements with the LHCb detector at the LHC. J. Instrum. **7**, P01010 (2012). arXiv:1110.2866
29. S. van der Meer, Calibration of the effective beam height in the ISR. CERN-ISR-PO-68-31
30. M. Ferro-Luzzi, Proposal for an absolute luminosity determination in colliding beam experiments using vertex detection of beam-gas

interactions. Nucl. Instrum. Methods, Sect. A **553**, 388 (2005). CERN-PH-EP-2005-023
31. M. Pivk, F.R. Le Diberder, sPlot: a statistical tool to unfold data distributions. Nucl. Instrum. Methods, Sect. A **555**, 356 (2005). arXiv:physics/0402083
32. R. Aaij et al. (LHCb collaboration), Measurement of J/ψ production in pp collisions at $\sqrt{s} = 7$ TeV. Eur. Phys. J. C **71**, 1645 (2011). arXiv:1103.0423
33. N. Brambilla et al., Heavy quarkonium: progress, puzzles, and opportunities. Eur. Phys. J. C **71**, 1534 (2011). arXiv:1010.5827

The LHCb Collaboration

R. Aaij[23], C. Abellan Beteta[35,n], B. Adeva[36], M. Adinolfi[42], C. Adrover[6], A. Affolder[48], Z. Ajaltouni[5], J. Albrecht[37], F. Alessio[37], M. Alexander[47], G. Alkhazov[29], P. Alvarez Cartelle[36], A.A. Alves Jr[22], S. Amato[2], Y. Amhis[38], J. Anderson[39], R.B. Appleby[50], O. Aquines Gutierrez[10], F. Archilli[18,37], L. Arrabito[53,p], A. Artamonov[34], M. Artuso[52,37], E. Aslanides[6], G. Auriemma[22,m], S. Bachmann[11], J.J. Back[44], D.S. Bailey[50], V. Balagura[30,37], W. Baldini[16], R.J. Barlow[50], C. Barschel[37], S. Barsuk[7], W. Barter[43], A. Bates[47], C. Bauer[10], Th. Bauer[23], A. Bay[38], I. Bediaga[1], S. Belogurov[30], K. Belous[34], I. Belyaev[30,37], E. Ben-Haim[8], M. Benayoun[8], G. Bencivenni[18], S. Benson[46], J. Benton[42], R. Bernet[39], M.-O. Bettler[17], M. van Beuzekom[23], A. Bien[11], S. Bifani[12], T. Bird[50], A. Bizzeti[17,h], P.M. Bjørnstad[50], T. Blake[37], F. Blanc[38], C. Blanks[49], J. Blouw[11], S. Blusk[52], A. Bobrov[33], V. Bocci[22], A. Bondar[33], N. Bondar[29], W. Bonivento[15], S. Borghi[47,50], A. Borgia[52], T.J.V. Bowcock[48], C. Bozzi[16], T. Brambach[9], J. van den Brand[24], J. Bressieux[38], D. Brett[50], M. Britsch[10], T. Britton[52], N.H. Brook[42], H. Brown[48], A. Büchler-Germann[39], I. Burducea[28], A. Bursche[39], J. Buytaert[37], S. Cadeddu[15], O. Callot[7], M. Calvi[20,j], M. Calvo Gomez[35,n], A. Camboni[35], P. Campana[18,37], A. Carbone[14], G. Carboni[21,k], R. Cardinale[19,37,i], A. Cardini[15], L. Carson[49], K. Carvalho Akiba[2], G. Casse[48], M. Cattaneo[37], Ch. Cauet[9], M. Charles[51], Ph. Charpentier[37], N. Chiapolini[39], K. Ciba[37], X. Cid Vidal[36], G. Ciezarek[49], P.E.L. Clarke[46,37], M. Clemencic[37], H.V. Cliff[43], J. Closier[37], C. Coca[28], V. Coco[23], J. Cogan[6], P. Collins[37], A. Comerma-Montells[35], F. Constantin[28], A. Contu[51], A. Cook[42], M. Coombes[42], G. Corti[37], G.A. Cowan[38], R. Currie[46], C. D'Ambrosio[37], P. David[8], P.N.Y. David[23], I. De Bonis[4], S. De Capua[21,k], M. De Cian[39], F. De Lorenzi[12], J.M. De Miranda[1], L. De Paula[2], P. De Simone[18], D. Decamp[4], M. Deckenhoff[9], H. Degaudenzi[38,37], L. Del Buono[8], C. Deplano[15], D. Derkach[14,37], O. Deschamps[5], F. Dettori[24], J. Dickens[43], H. Dijkstra[37], P. Diniz Batista[1], F. Domingo Bonal[35,n], S. Donleavy[48], F. Dordei[11], A. Dosil Suárez[36], D. Dossett[44], A. Dovbnya[40], F. Dupertuis[38], R. Dzhelyadin[34], A. Dziurda[25], S. Easo[45], U. Egede[49], V. Egorychev[30], S. Eidelman[33], D. van Eijk[23], F. Eisele[11], S. Eisenhardt[46], R. Ekelhof[9], L. Eklund[47], Ch. Elsasser[39], D. Elsby[55], D. Esperante Pereira[36], L. Estève[43], A. Falabella[16,14,e], E. Fanchini[20,j], C. Färber[11], G. Fardell[46], C. Farinelli[23], S. Farry[12], V. Fave[38], V. Fernandez Albor[36], M. Ferro-Luzzi[37], S. Filippov[32], C. Fitzpatrick[46], M. Fontana[10], F. Fontanelli[19,i], R. Forty[37], M. Frank[37], C. Frei[37], M. Frosini[17,37,f], S. Furcas[20], A. Gallas Torreira[36], D. Galli[14,c], M. Gandelman[2], P. Gandini[51], Y. Gao[3], J-C. Garnier[37], J. Garofoli[52], J. Garra Tico[43], L. Garrido[35], D. Gascon[35], C. Gaspar[37], N. Gauvin[38], M. Gersabeck[37], T. Gershon[44,37], Ph. Ghez[4], V. Gibson[43], V.V. Gligorov[37], C. Göbel[54,q], D. Golubkov[30], A. Golutvin[49,30,37], A. Gomes[2], H. Gordon[51], M. Grabalosa Gándara[35], R. Graciani Diaz[35], L.A. Granado Cardoso[37], E. Graugés[35], G. Graziani[17], A. Grecu[28], E. Greening[51], S. Gregson[43], B. Gui[52], E. Gushchin[32], Yu. Guz[34], T. Gys[37], G. Haefeli[38], C. Haen[37], S.C. Haines[43], T. Hampson[42], S. Hansmann-Menzemer[11], R. Harji[49], N. Harnew[51], J. Harrison[50], P.F. Harrison[44], T. Hartmann[56,r], J. He[7], V. Heijne[23], K. Hennessy[48], P. Henrard[5], J.A. Hernando Morata[36], E. van Herwijnen[37], E. Hicks[48], K. Holubyev[11], P. Hopchev[4], W. Hulsbergen[23], P. Hunt[51], T. Huse[48], R.S. Huston[12], D. Hutchcroft[48], D. Hynds[47], V. Iakovenko[41], P. Ilten[12], J. Imong[42], R. Jacobsson[37], A. Jaeger[11], M. Jahjah Hussein[5], E. Jans[23], F. Jansen[23], P. Jaton[38], B. Jean-Marie[7], F. Jing[3], M. John[51], D. Johnson[51], C.R. Jones[43], B. Jost[37], M. Kaballo[9], S. Kandybei[40], M. Karacson[37], T.M. Karbach[9], J. Keaveney[12], I.R. Kenyon[55], U. Kerzel[37], T. Ketel[24], A. Keune[38], B. Khanji[6], Y.M. Kim[46], M. Knecht[38], P. Koppenburg[23], A. Kozlinskiy[23], L. Kravchuk[32], K. Kreplin[11], M. Kreps[44], G. Krocker[11], P. Krokovny[11], F. Kruse[9], K. Kruzelecki[37], M. Kucharczyk[20,25,37,j], T. Kvaratskheliya[30,37], V.N. La Thi[38], D. Lacarrere[37], G. Lafferty[50], A. Lai[15], D. Lambert[46], R.W. Lambert[24], E. Lanciotti[37], G. Lanfranchi[18], C. Langenbruch[11], T. Latham[44], C. Lazzeroni[55], R. Le Gac[6], J. van Leerdam[23], J.-P. Lees[4], R. Lefèvre[5], A. Leflat[31,37], J. Lefrançois[7], O. Leroy[6], T. Lesiak[25], L. Li[3], L. Li Gioi[5], M. Lieng[9], M. Liles[48], R. Lindner[37], C. Linn[11], B. Liu[3], G. Liu[37], J. von Loeben[20], J.H. Lopes[2], E. Lopez Asamar[35], N. Lopez-March[38], H. Lu[38,3], J. Luisier[38], A. Mac Raighne[47], F. Machefert[7], I.V. Machikhiliyan[4,30], F. Maciuc[10], O. Maev[29,37], J. Magnin[1], S. Malde[51], R.M.D. Mamunur[37], G. Manca[15,d], G. Mancinelli[6], N. Mangiafave[43], U. Marconi[14], R. Märki[38], J. Marks[11], G. Martellotti[22], A. Martens[8], L. Martin[51], A. Martín Sánchez[7], D. Martinez Santos[37], A. Massafferri[1], Z. Mathe[12], C. Matteuzzi[20], M. Matveev[29], E. Maurice[6],

B. Maynard[52], A. Mazurov[16,32,37], G. McGregor[50], R. McNulty[12], M. Meissner[11], M. Merk[23], J. Merkel[9], R. Messi[21,k], S. Miglioranzi[37], D.A. Milanes[13,37], M.-N. Minard[4], J. Molina Rodriguez[54,q], S. Monteil[5], D. Moran[12], P. Morawski[25], R. Mountain[52], I. Mous[23], F. Muheim[46], K. Müller[39], R. Muresan[28,38], B. Muryn[26], B. Muster[38], M. Musy[35], J. Mylroie-Smith[48], P. Naik[42], T. Nakada[38], R. Nandakumar[45], I. Nasteva[1], M. Nedos[9], M. Needham[46], N. Neufeld[37], C. Nguyen-Mau[38,o], M. Nicol[7], V. Niess[5], N. Nikitin[31], A. Nomerotski[51], A. Novoselov[34], A. Oblakowska-Mucha[26], V. Obraztsov[34], S. Oggero[23], S. Ogilvy[47], O. Okhrimenko[41], R. Oldeman[15,d], M. Orlandea[28], J.M. Otalora Goicochea[2], P. Owen[49], K. Pal[52], J. Palacios[39], A. Palano[13,b], M. Palutan[18], J. Panman[37], A. Papanestis[45], M. Pappagallo[47], C. Parkes[50,37], C.J. Parkinson[49], G. Passaleva[17], G.D. Patel[48], M. Patel[49], S.K. Paterson[49], G.N. Patrick[45], C. Patrignani[19,i], C. Pavel-Nicorescu[28], A. Pazos Alvarez[36], A. Pellegrino[23], G. Penso[22,l], M. Pepe Altarelli[37], S. Perazzini[14,c], D.L. Perego[20,j], E. Perez Trigo[36], A. Pérez-Calero Yzquierdo[35], P. Perret[5], M. Perrin-Terrin[6], G. Pessina[20], A. Petrella[16,37], A. Petrolini[19,i], A. Phan[52], E. Picatoste Olloqui[35], B. Pie Valls[35], B. Pietrzyk[4], T. Pilař[44], D. Pinci[22], R. Plackett[47], S. Playfer[46], M. Plo Casasus[36], G. Polok[25], A. Poluektov[44,33], E. Polycarpo[2], D. Popov[10], B. Popovici[28], C. Potterat[35], A. Powell[51], J. Prisciandaro[38], V. Pugatch[41], A. Puig Navarro[35], W. Qian[52], J.H. Rademacker[42], B. Rakotomiaramanana[38], M.S. Rangel[2], I. Raniuk[40], G. Raven[24], S. Redford[51], M.M. Reid[44], A.C. dos Reis[1], S. Ricciardi[45], K. Rinnert[48], D.A. Roa Romero[5], P. Robbe[7], E. Rodrigues[47,50], F. Rodrigues[2], P. Rodriguez Perez[36], G.J. Rogers[43], S. Roiser[37], V. Romanovsky[34], M. Rosello[35,n], J. Rouvinet[38], T. Ruf[37], H. Ruiz[35], G. Sabatino[21,k], J.J. Saborido Silva[36], N. Sagidova[29], P. Sail[47], B. Saitta[15,d], C. Salzmann[39], M. Sannino[19,i], R. Santacesaria[22], C. Santamarina Rios[36], R. Santinelli[37], E. Santovetti[21,k], M. Sapunov[6], A. Sarti[18,l], C. Satriano[22,m], A. Satta[21], M. Savrie[16,e], D. Savrina[30], P. Schaack[49], M. Schiller[24], S. Schleich[9], M. Schlupp[9], M. Schmelling[10], B. Schmidt[37], O. Schneider[38], A. Schopper[37], M.-H. Schune[7], R. Schwemmer[37], B. Sciascia[18], A. Sciubba[18,l], M. Seco[36], A. Semennikov[30], K. Senderowska[26], I. Sepp[49], N. Serra[39], J. Serrano[6], P. Seyfert[11], M. Shapkin[34], I. Shapoval[40,37], P. Shatalov[30], Y. Shcheglov[29], T. Shears[48], L. Shekhtman[33], O. Shevchenko[40], V. Shevchenko[30], A. Shires[49], R. Silva Coutinho[44], T. Skwarnicki[52], A.C. Smith[37], N.A. Smith[48], E. Smith[51,45], K. Sobczak[5], F.J.P. Soler[47], A. Solomin[42], F. Soomro[18], B. Souza De Paula[2], B. Spaan[9], A. Sparkes[46], P. Spradlin[47], F. Stagni[37], S. Stahl[11], O. Steinkamp[39], S. Stoica[28], S. Stone[52,37], B. Storaci[23], M. Straticiuc[28], U. Straumann[39], V.K. Subbiah[37], S. Swientek[9], M. Szczekowski[27], P. Szczypka[38], T. Szumlak[26], S. T'Jampens[4], E. Teodorescu[28], F. Teubert[37], C. Thomas[51], E. Thomas[37], J. van Tilburg[11], V. Tisserand[4], M. Tobin[39], S. Topp-Joergensen[51], N. Torr[51], E. Tournefier[4,49], M.T. Tran[38], A. Tsaregorodtsev[6], N. Tuning[23], M. Ubeda Garcia[37], A. Ukleja[27], P. Urquijo[52], U. Uwer[11], V. Vagnoni[14], G. Valenti[14], R. Vazquez Gomez[35], P. Vazquez Regueiro[36], S. Vecchi[16], J.J. Velthuis[42], M. Veltri[17,g], B. Viaud[7], I. Videau[7], X. Vilasis-Cardona[35,n], J. Visniakov[36], A. Vollhardt[39], D. Volyanskyy[10], D. Voong[42], A. Vorobyev[29], H. Voss[10], S. Wandernoth[11], J. Wang[52], D.R. Ward[43], N.K. Watson[55], A.D. Webber[50], D. Websdale[49], M. Whitehead[44], D. Wiedner[11], L. Wiggers[23], G. Wilkinson[51], M.P. Williams[44,45], M. Williams[49], F.F. Wilson[45], J. Wishahi[9], M. Witek[25], W. Witzeling[37], S.A. Wotton[43], K. Wyllie[37], Y. Xie[46], F. Xing[51], Z. Xing[52], Z. Yang[3], R. Young[46], O. Yushchenko[34], M. Zavertyaev[10,a], F. Zhang[3], L. Zhang[52], W.C. Zhang[12], Y. Zhang[3], A. Zhelezov[11], L. Zhong[3], E. Zverev[31], A. Zvyagin[37]

[1]Centro Brasileiro de Pesquisas Físicas (CBPF), Rio de Janeiro, Brazil
[2]Universidade Federal do Rio de Janeiro (UFRJ), Rio de Janeiro, Brazil
[3]Center for High Energy Physics, Tsinghua University, Beijing, China
[4]LAPP, Université de Savoie, CNRS/IN2P3, Annecy-Le-Vieux, France
[5]Clermont Université, Université Blaise Pascal, CNRS/IN2P3, LPC, Clermont-Ferrand, France
[6]CPPM, Aix-Marseille Université, CNRS/IN2P3, Marseille, France
[7]LAL, Université Paris-Sud, CNRS/IN2P3, Orsay, France
[8]LPNHE, Université Pierre et Marie Curie, Université Paris Diderot, CNRS/IN2P3, Paris, France
[9]Fakultät Physik, Technische Universität Dortmund, Dortmund, Germany
[10]Max-Planck-Institut für Kernphysik (MPIK), Heidelberg, Germany
[11]Physikalisches Institut, Ruprecht-Karls-Universität Heidelberg, Heidelberg, Germany
[12]School of Physics, University College Dublin, Dublin, Ireland
[13]Sezione INFN di Bari, Bari, Italy
[14]Sezione INFN di Bologna, Bologna, Italy
[15]Sezione INFN di Cagliari, Cagliari, Italy
[16]Sezione INFN di Ferrara, Ferrara, Italy
[17]Sezione INFN di Firenze, Firenze, Italy
[18]Laboratori Nazionali dell'INFN di Frascati, Frascati, Italy
[19]Sezione INFN di Genova, Genova, Italy
[20]Sezione INFN di Milano Bicocca, Milano, Italy

[21]Sezione INFN di Roma Tor Vergata, Roma, Italy
[22]Sezione INFN di Roma La Sapienza, Roma, Italy
[23]Nikhef National Institute for Subatomic Physics, Amsterdam, The Netherlands
[24]Nikhef National Institute for Subatomic Physics and Vrije Universiteit, Amsterdam, The Netherlands
[25]Henryk Niewodniczanski Institute of Nuclear Physics Polish Academy of Sciences, Kraców, Poland
[26]AGH University of Science and Technology, Kraców, Poland
[27]Soltan Institute for Nuclear Studies, Warsaw, Poland
[28]Horia Hulubei National Institute of Physics and Nuclear Engineering, Bucharest-Magurele, Romania
[29]Petersburg Nuclear Physics Institute (PNPI), Gatchina, Russia
[30]Institute of Theoretical and Experimental Physics (ITEP), Moscow, Russia
[31]Institute of Nuclear Physics, Moscow State University (SINP MSU), Moscow, Russia
[32]Institute for Nuclear Research of the Russian Academy of Sciences (INR RAN), Moscow, Russia
[33]Budker Institute of Nuclear Physics (SB RAS) and Novosibirsk State University, Novosibirsk, Russia
[34]Institute for High Energy Physics (IHEP), Protvino, Russia
[35]Universitat de Barcelona, Barcelona, Spain
[36]Universidad de Santiago de Compostela, Santiago de Compostela, Spain
[37]European Organization for Nuclear Research (CERN), Geneva, Switzerland
[38]Ecole Polytechnique Fédérale de Lausanne (EPFL), Lausanne, Switzerland
[39]Physik-Institut, Universität Zürich, Zürich, Switzerland
[40]NSC Kharkiv Institute of Physics and Technology (NSC KIPT), Kharkiv, Ukraine
[41]Institute for Nuclear Research of the National Academy of Sciences (KINR), Kyiv, Ukraine
[42]H.H. Wills Physics Laboratory, University of Bristol, Bristol, United Kingdom
[43]Cavendish Laboratory, University of Cambridge, Cambridge, United Kingdom
[44]Department of Physics, University of Warwick, Coventry, United Kingdom
[45]STFC Rutherford Appleton Laboratory, Didcot, United Kingdom
[46]School of Physics and Astronomy, University of Edinburgh, Edinburgh, United Kingdom
[47]School of Physics and Astronomy, University of Glasgow, Glasgow, United Kingdom
[48]Oliver Lodge Laboratory, University of Liverpool, Liverpool, United Kingdom
[49]Imperial College London, London, United Kingdom
[50]School of Physics and Astronomy, University of Manchester, Manchester, United Kingdom
[51]Department of Physics, University of Oxford, Oxford, United Kingdom
[52]Syracuse University, Syracuse, NY, United States
[53]CC-IN2P3, CNRS/IN2P3, Lyon-Villeurbanne, France
[54]Pontifícia Universidade Católica do Rio de Janeiro (PUC-Rio), Rio de Janeiro, Brazil
[55]University of Birmingham, Birmingham, United Kingdom
[56]Physikalisches Institut, Universität Rostock, Rostock, Germany
[a]P.N. Lebedev Physical Institute, Russian Academy of Science (LPI RAS), Moscow, Russia
[b]Università di Bari, Bari, Italy
[c]Università di Bologna, Bologna, Italy
[d]Università di Cagliari, Cagliari, Italy
[e]Università di Ferrara, Ferrara, Italy
[f]Università di Firenze, Firenze, Italy
[g]Università di Urbino, Urbino, Italy
[h]Università di Modena e Reggio Emilia, Modena, Italy
[i]Università di Genova, Genova, Italy
[j]Università di Milano Bicocca, Milano, Italy
[k]Università di Roma Tor Vergata, Roma, Italy
[l]Università di Roma La Sapienza, Roma, Italy
[m]Università della Basilicata, Potenza, Italy
[n]LIFAELS, La Salle, Universitat Ramon Llull, Barcelona, Spain
[o]Hanoi University of Science, Hanoi, Viet Nam
[p]Associated member
[q]Associated to Universidade Federal do Rio de Janeiro (UFRJ), Rio de Janeiro, Brazil
[r]Associated to Physikalisches Institut, Ruprecht-Karls-Universität Heidelberg, Heidelberg, Germany